Video Article

Development of Whispering Gallery Mode Polymeric Micro-optical Electric Field Sensors

Tindaro Ioppolo[1], Volkan Ötügen[1], Ulas Ayaz[1]

[1]Mechanical Engineering Department, Southern Methodist University

Correspondence to: Volkan Ötügen at otugen@engr.smu.edu

URL: https://www.jove.com/video/50199
DOI: doi:10.3791/50199

Keywords: Mechanical Engineering, Issue 71, Physics, Optics, Materials Science, Chemical Engineering, electrostatics, optical fibers, optical materials, optical waveguides, optics, optoelectronics, photonics, geometrical optics, sensors, electric field, dielectric resonators, micro-spheres, whispering gallery mode, morphology dependent resonance, PDMS

Date Published: 1/29/2013

Citation: Ioppolo, T., Ötügen, V., Ayaz, U. Development of Whispering Gallery Mode Polymeric Micro-optical Electric Field Sensors. *J. Vis. Exp.* (71), e50199, doi:10.3791/50199 (2013).

Abstract

Optical modes of dielectric micro-cavities have received significant attention in recent years for their potential in a broad range of applications. The optical modes are frequently referred to as "whispering gallery modes" (WGM) or "morphology dependent resonances" (MDR) and exhibit high optical quality factors. Some proposed applications of micro-cavity optical resonators are in spectroscopy[1], micro-cavity laser technology[2], optical communications[3-6] as well as sensor technology. The WGM-based sensor applications include those in biology[7], trace gas detection[8], and impurity detection in liquids[9]. Mechanical sensors based on microsphere resonators have also been proposed, including those for force[10,11], pressure[12], acceleration[13] and wall shear stress[14]. In the present, we demonstrate a WGM-based electric field sensor, which builds on our previous studies[15,16]. A candidate application of this sensor is in the detection of neuronal action potential.

The electric field sensor is based on polymeric multi-layered dielectric microspheres. The external electric field induces surface and body forces on the spheres (electrostriction effect) leading to elastic deformation. This change in the morphology of the spheres, leads to shifts in the WGM. The electric field-induced WGM shifts are interrogated by exciting the optical modes of the spheres by laser light. Light from a distributed feedback (DFB) laser (nominal wavelength of ~ 1.3 μm) is side-coupled into the microspheres using a tapered section of a single mode optical fiber. The base material of the spheres is polydimethylsiloxane (PDMS). Three microsphere geometries are used: (1) PDMS sphere with a 60:1 volumetric ratio of base-to-curing agent mixture, (2) multi layer sphere with 60:1 PDMS core, in order to increase the dielectric constant of the sphere, a middle layer of 60:1 PDMS that is mixed with varying amounts (2% to 10% by volume) of barium titanate and an outer layer of 60:1 PDMS and (3) solid silica sphere coated with a thin layer of uncured PDMS base. In each type of sensor, laser light from the tapered fiber is coupled into the outermost layer that provides high optical quality factor WGM (Q ~ 10^6). The microspheres are poled for several hours at electric fields of ~ 1 MV/m to increase their sensitivity to electric field.

Video Link

The video component of this article can be found at https://www.jove.com/video/50199/

Protocol

1. PDMS Microsphere Preparation (Sphere I)

1. Polydimethylsiloxane (PDMS) base and the curing agent are mixed with a volume ratio of 60:1.
2. A strand of silica optical fiber, about 2 cm long, is first stripped of its plastic cladding using an optical stripper.
3. One end of the fiber is heated and stretched to provide a stem end that is ~25-50 μm in diameter at the tip.
4. The stretched end of the fiber is submerged into the PDMS mixture by a length of approximately 2-4 mm and then is pulled out.
5. Surface tension and weight of the PDMS mixture allow for the formation of a sphere at the tip of the silica fiber. The size of the sphere is controlled by the dipping length and extraction velocity. By varying these two parameters, sphere diameters in the range 100 μm - 1,000 μm can be obtained.
6. The microsphere/stem assembly is then placed in an oven at ~90 °C for 4 hr to allow for proper curing of the polymer material (to form cross-linked chains). **Figure 1a** is a schematic of Sphere I.

2. PDMS-based Triple Layer Sphere Preparation (Sphere II)

1. A 60:1 PDMS microsphere is used as the inner core. The same steps described in 1) above is followed for this process.
2. A mixture of barium titanate ($BaTiO_3$) nano-particles and 60:1 PDMS is used as the middle layer. The PDMS mixture, prepared in the same way described in 1.1) above, is mixed with barium titanate nano-particles.

3. The PDMS microsphere core described in 2.1) is then dipped into the PDMS- barium titanate mixture to coat it (with a layer nominal thickness of ~ 10 μm).
4. Next, the two-layer sphere is placed in an oven at ~ 90 °C for 4 hr to allow for proper curing of the second layer.
5. Once the two layer sphere is cured, it is again immersed in a mixture of 60:1 PDMS to provide an outer coating (third layer). This outermost layer serves as spherical optical guide (~10 μm thickness). **Figure 1b** is a schematic of Sphere II.

3. Silica/PDMS Microsphere Preparation (Sphere III)

1. A ~ 3 cm long section of a silica single mode optical fiber is first stripped of its buffer (plastic) coating and then its tip is melted using a micro-torch (together with the cladding and core). Surface tension and gravity work together to shape the melted tip into a sphere. Spheres with diameters ranging from 200 to 500 μm can be obtained with this process.
2. The silica microsphere is then immersed in a bath of PDMS base (without the curing agent) to cover it with a coat of ~ 50 μm. This outer layer stays as a highly-viscous Bingham (yield-stress) fluid. **Figure 1c** is a schematic of Sphere III.

4. Optical Fiber Preparation

1. A section of a single mode optical fiber is stripped of its plastic cladding using an optical stripper. Using a micro-torch the striped section of the fiber is heated until it is molten (both the cladding and fiber core).
2. While the middle section is molten, one end of the optical fiber is pulled along its axis to form a tapered section of the fiber that is about 1 cm long. The duration of heating, the pulling speed and distance determine the diameter of the tapered section that ranges between 10 and 20 μm. The light from the DFB laser is coupled into the sphere through the tapered section of the fiber. **Figure 2** shows the sphere-fiber coupling.

5. Optoelectronic Setup

1. The output of a tunable DFB laser is coupled into a single mode optical fiber on one end and terminated at a fast photodiode on the other end as shown in **Figure 3**.
2. The photodiode output is digitized using an analog-to-digital converter (A/D) and stored on a personal computer (PC).
3. Using a micro-translation stage the microsphere (Type I, II or III) is brought in contact with the tapered section of the optical fiber (**Figures 2** and **3**) to provide optical coupling between the two elements.
4. The DFB laser is tuned by a laser controller. The laser controller, in turn is driven by a function generator which provides a saw-tooth voltage input.

6. Electric Field Generation

1. Two square brass plates (2 x 2 cm) with thickness of 1 mm are used to generate the uniform electric field. The plates are connected to a voltage supply and the sphere sensors are placed in the gap between the two plates (**Figure 4**).
2. In order to increase the measurement sensitivity, the spheres are first poled in an electric field of 1 MV/m for 2 hr.

Representative Results

An optical mode (WGM) of the sphere is excited by the laser light when optical path length traveled by the light is a multiple integer of the laser wavelength. For the arrangement shown in **Figure 3**, the optical path length is $2\pi rn$, where n and r are the refractive index and radius of the sphere, respectively. Using geometric optics approximation, a WGM condition is satisfied when $2\pi rn = l\lambda$ where l is an integer and λ is the laser's wavelength. As the DFB laser is tuned across a small wavelength range, the dielectric sphere's optical modes (WGM) are seen as sharp dips in the spectrum through the optical fiber. When the sphere undergoes an elastic deformation due to the external electric field, the position of a dip in the transmission spectrum shifts. **Figure 5** shows typical transmission spectra and the WGM shift due to external electric field for a 60:1 PDMS sphere of 900 μm diameter. When the electric field of 50 kV/m is turned on, the WGM optical mode, seen as a dip in the transmission spectrum, experiences a blue-shift of $\Delta\lambda \approx 1.9$ pm indicating that the sphere is elongated along the field direction. Note that the optical path length inside the sphere is on the equatorial plane normal to the electric field direction (**Figure 4**). The optical quality factor for the WGM dip in the figure is $\sim 5 \times 10^5$.

Figure 6a shows the WGM shift, $\Delta\lambda$, of Sphere I under 1 Hz harmonic electric field with amplitude of 200 V/m. The sphere diameter is 700 μm and it is poled for 2 hr in a static electric field of 1 MV/m. The corresponding WGM shift vs electric field amplitude plot is shown in **Figure 6b**. Sphere I yields a sensitivity of 1.7 pm/(kV/m). The results for Sphere II and III are shown in **Figures 7** and **8**, respectively. **Figure 7** shows the results of Sphere II with outer diameter ~700 μm and **Figure 8** display the measurement with Sphere III which consisted of 300 μm silica core and 150 μm thickness of PDMS base coated over it. In these measurements, the Q-factors ranged from 5×10^5 to 10^6. The sphere morphology and the associated WGM are sensitive to other external conditions. Thus, each measurement is completed in a short period of time (~1 min) so that, the environmental effects (such as temperature, humidity etc.) on WGM shifts are negligible.

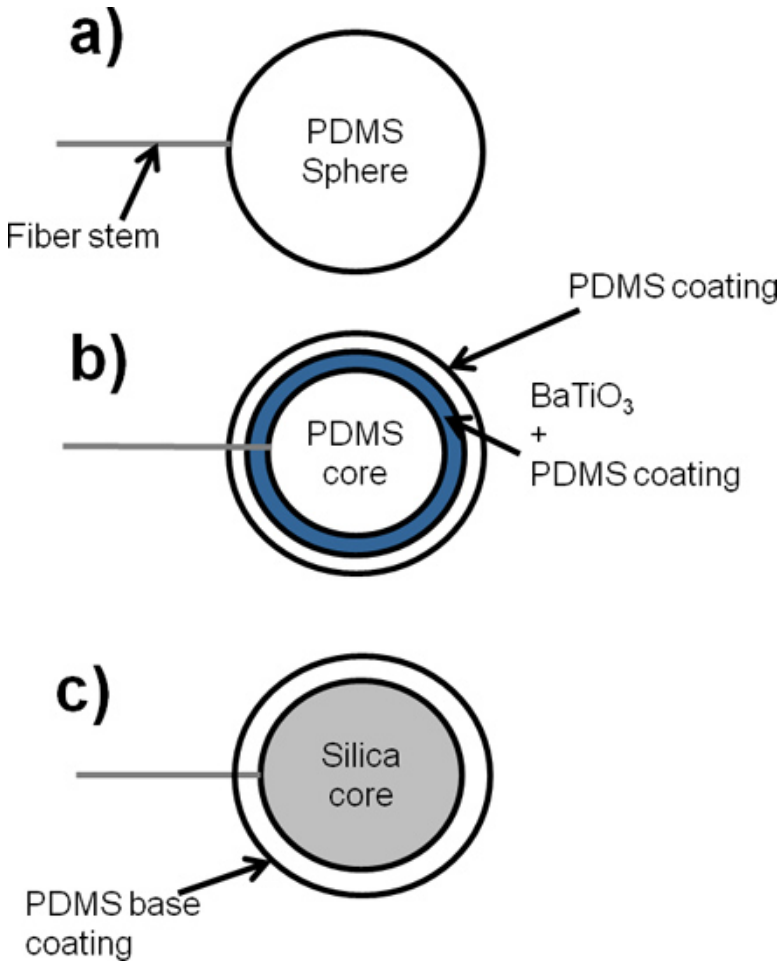

Figure 1. Schematic of the three sphere sensor configurations.

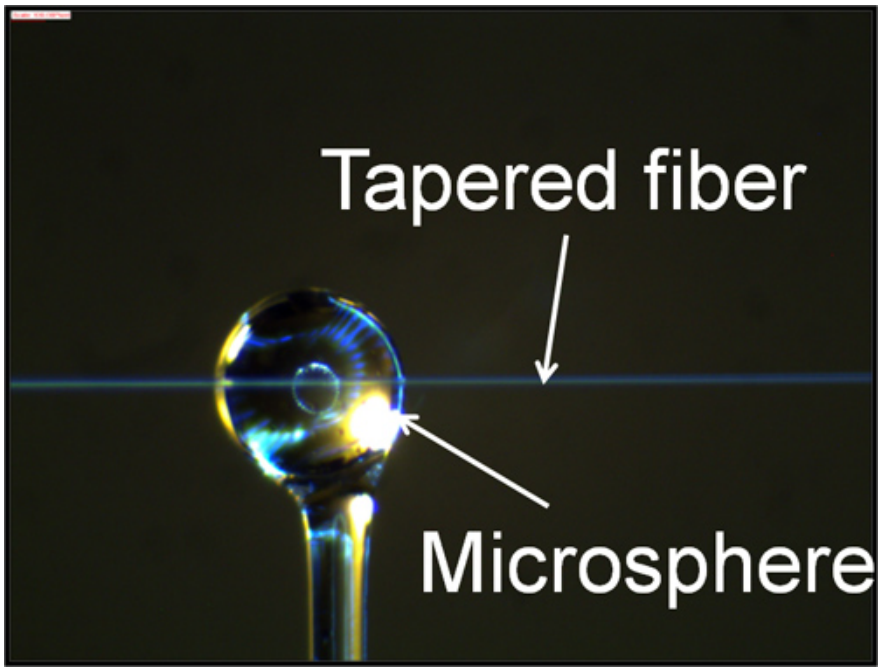

Figure 2. Photograph of coupled sphere-tapered fiber.

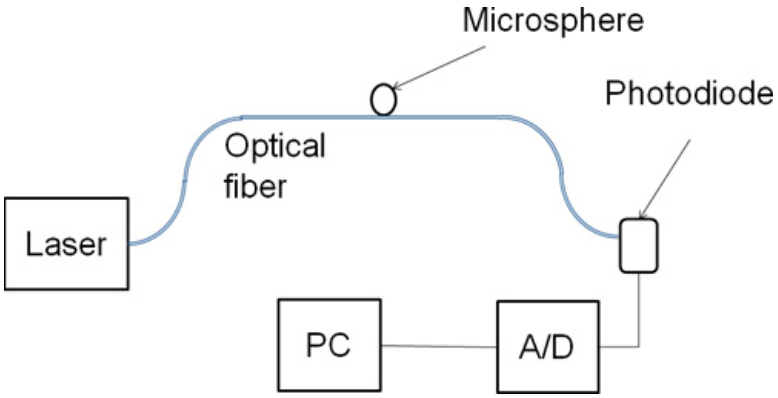

Figure 3. Schematic of optoelectronic setup.

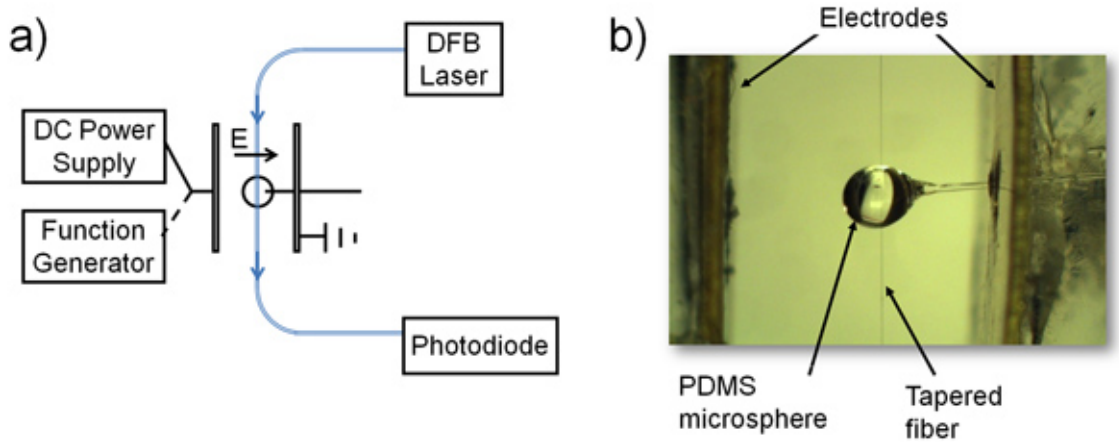

Figure 4. Schematic (a); photograph (b) of the experimental setup.

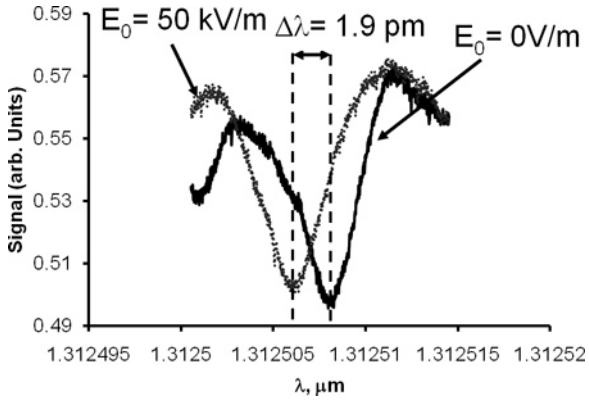

Figure 5. Transmission spectra through the sphere-coupled fiber.

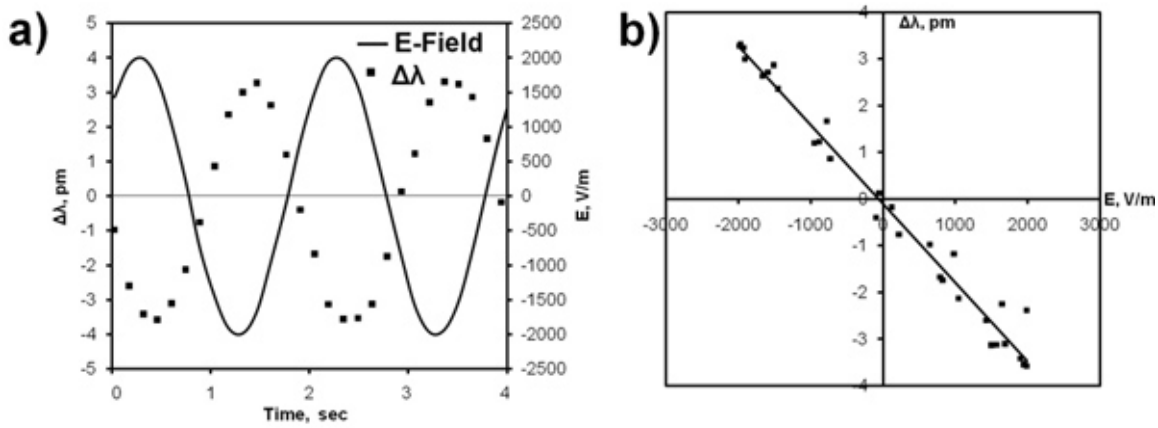

Figure 6. WGM shift of Sphere I under harmonic field perturbation (a); WGM shift vs electric field amplitude (b). Click here to view larger figure.

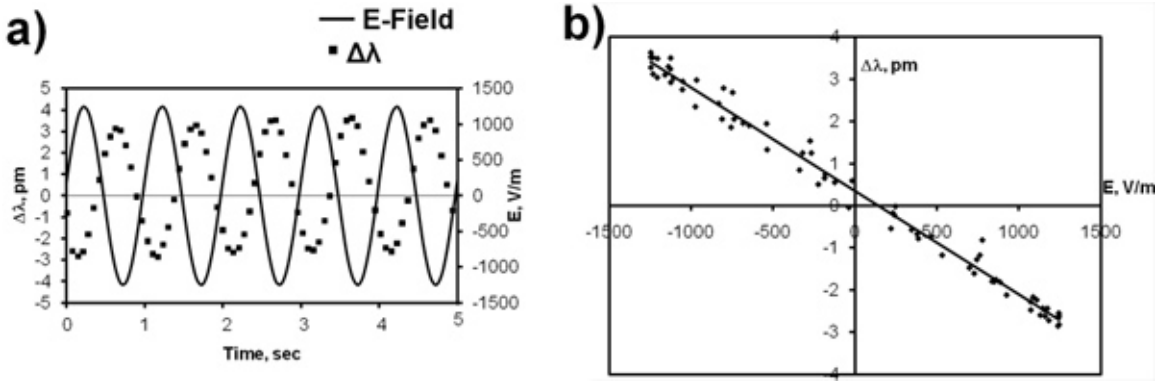

Figure 7. WGM shift of Sphere II under harmonic field perturbation (a); WGM shift vs electric field amplitude (b). Click here to view larger figure.

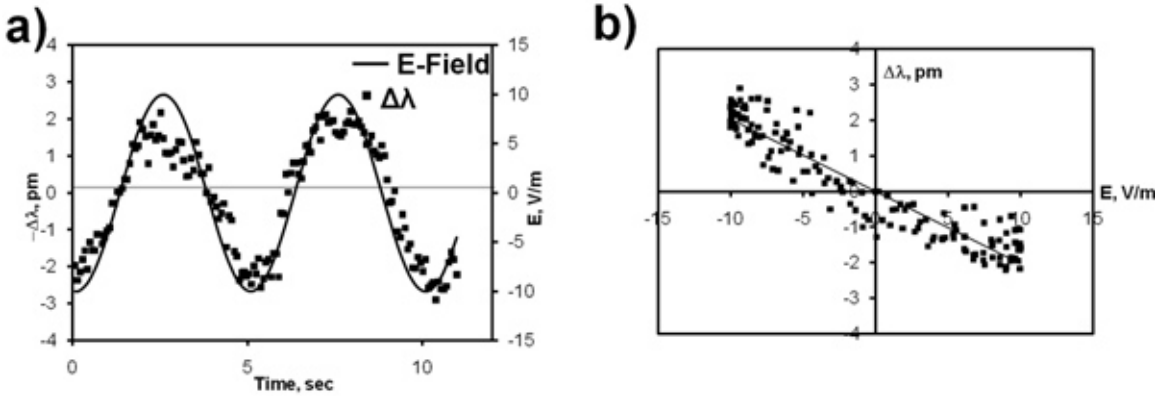

Figure 8. WGM shift of Sphere III under harmonic field perturbation (a); WGM shift vs electric field amplitude (b). Click here to view larger figure.

Discussion

The spheres are initially poled by connecting the electrodes to a DC high voltage supply. At the end of the poling duration, the electrode leads are disconnected from the DC voltage supply and connected to a function generator as indicated in **Figure 4**. The results presented in **Figures 5** through **8** show that positive and negative electric fields (relative to direction of poling) lead to sphere elongation and compression, respectively. Sphere I, which is a single layer 60:1 PDMS has an electric field sensitivity of 1.7 pm/(kV/m). Significant improvement in sensitivity is obtained by using multi-layer spheres. Sphere II provides electric field sensitivity of 2.5 pm/(kV/m). Yet a much higher sensitivity is obtained with Sphere III (~ 0.2 pm/(V/m) due to the soft , yield stress-liquid outer layer. With a conservative assumption that the minimum measurable WGM shift is $\delta\lambda = \lambda/Q$, typical WGM sensor resolution can be expressed as

$$\delta E_o = \frac{\lambda}{Q}\left(\frac{d\lambda}{dE_o}\right)^{-1}$$

where E_o is the applied electric field. Sensor resolution given in the above equation can be further improved by utilizing better signal processing methods. For example, the signal processing method described in our recent study[17] provides a shift detection resolution of ~0.13 pm. For our studies, this is equivalent to having a sensor *Q*-factor of 10^7 in the above equation for sensor resolution.

These results are encouraging for future development of WGM-based micro-optical sensors. A particular application is an all optical, fiber-based neurophotonic interface.

Disclosures

We have nothing to disclose.

Acknowledgements

This research is sponsored by the US Defense Advanced Research Projects Agency under Centers in Integrated Photonics Engineering Research (CIPhER) program with Dr. J. Scott Rodgers as project manager. The information provided in this report does not necessarily reflect the position or the policy of the US Government and no official endorsement should be inferred.

References

1. von Klitzing, W. Tunable whispering gallery modes for spectroscopy and CQED experiments. *New journal of physics.* **3**, 14.1-14.14 (2001).
2. Cai, M., Painter, O., Vahala, K.J., & Sercel, P.C. Fiber-coupled microsphere laser. *Optics letters.* **25** (19), 1430-1432 (2000).
3. Tapalian, H.C., Laine, J.P., & Lane, P.A. Thermooptical switches using coated microsphere resonators. *IEEE photonics technology letters.* **14** (8), 1118-1120 (2002).
4. Little, B.E., Chu, S.T., & Haus, H.A. Microring resonator channel dropping filters. *Journal of lightwave technology.* **15**, 998-1000 (1997).
5. Offrein, B.J., Germann, R., Horst, F., Salemink, H.W.M., Beyerl, R., & Bona, G.L. Resonant coupler-based tunable add-after-drop filter in silicon-oxynitride technology for WDM networks. *IEEE journal of selected topics in quantum electronics.* **5**, 1400-1406 (1999).
6. Ilchenko, V.S., Volikov, P.S., *et al.* Strain tunable high-*Q* optical microsphere resonator. *Optics communications.* **145**, 86-90 (1998).
7. Arnold, S., Khoshsima, M., Teraoka, I., Holler, S., & Vollmer, F. Shift of whispering-gallery modes in microspheres by protein adsorption. *Optics letters.* **28** (4), 272-274 (2003).
8. Rosenberger, A.T. & Rezac, J.P. Whispering-gallery mode evanescent-wave microsensor for trace-gas detection. *Proceedings of SPIE.* **4265**, 102-112 (2001).
9. Ioppolo, T., Das, N., & Ötügen, M.V. Whispering gallery modes of microspheres in the presence of a changing surrounding medium: A new ray-tracing analysis and sensor experiment. *Journal of applied physics.* **107**, 103105 (2010).
10. Ioppolo, T., Ayaz, U.K., & Ötügen, M.V. High-resolution force sensor based on morphology dependent optical resonances of polymeric spheres. *Journal of applied physics.* **105** (1), 013535 (2009).
11. Ioppolo, T., Kozhevnikov, M., Stepaniuk, V., Ötügen, M.V., & Sheverev, V. Micro-optical force sensor concept based on whispering gallery mode resonances. *Applied optics.* **47** (16), 3009-3014 (2008).
12. Ioppolo, T. & Ötügen, M.V. Pressure tuning of whispering gallery mode resonators. *Journal of optical society of America B.* **24** (10), 2721-2726 (2007).
13. Ioppolo, T. & Ötügen, M.V. Effect of acceleration on the morphology dependent optical resonances of spherical resonators. *Journal of optical society of America B.* **28**, 225-227 (2011).
14. Ayaz, U.K., Ioppolo, T., & Ötügen, M.V. Wall shear stress sensor based on the optical resonances of dielectric microspheres. *Measurement science and technology.* **22**, 075203 (2011).
15. Ioppolo, T., Ayaz, U.K., & Ötügen, M.V. Tuning of whispering gallery modes of spherical resonators using an external electric field. *Optics express.* **17** (19), 16465-16479 (2009).
16. Ioppolo, T., Stubblefield, J., & Ötügen, M.V., Electric field-induced deformation of polydimethylsiloxane polymers. *Journal of applied physics.* **112**, 044906 (2012).
17. Manzo, M., Ioppolo, T., Ayaz, U.K., LaPenna, V., & Ötügen, M.V. A photonic wall pressure sensor for fluid mechanics applications. *Review of scientific instrumentation.* **83**, 105003 (2012).

